IEICE Communications Express, Vol.13, No.3, 52–55

ComEX

LETTER

Resource allocation for hybrid FSO/RF satellite-assisted multiple backhauled UAVs over Starlink networks

Khanh D. Dang[1], **Hoang D. Le**[2, a)], **Chuyen T. Nguyen**[1], **and Anh T. Pham**[2]

Abstract This letter addresses the resource allocation issue for hybrid free-space optics (FSO)/radio frequency (RF)-based satellite-assisted multiple users. Specifically, we present the rate adaptation-aided data frame allocation design for hybrid FSO/RF satellite-assisted multiple unmanned aerial vehicles (UAVs). The considered allocation scheme ensures latency fairness among UAVs serving as flying base stations (BSs). Numerical results confirm the effectiveness of the proposed solution over the state-of-the-art. Moreover, we investigate the feasibility of a case study over the Japan networks using practical SpaceX's Starlink satellite constellation.

Keywords: hybrid FSO/RF links, satellite communications, rate adaptation, data frame allocation, multiple UAVs

Classification: Satellite communications

1. Introduction

To realize seamless coverage and extremely high achievable throughput, the integration of non-terrestrial networks (NTNs) and hybrid free-space optical (FSO)/radio frequency (RF) communications has emerged as a promising solution for future 6G wireless networks [1]. As released by the 3rd Generation Partnership Project (3GPP), NTN includes satellites and networked flying platforms (NFPs), which offer wide-area coverage, scalability, flexible deployment, and cost-effectiveness [2]. On the other hand, by integrating technological benefits and the prevention of defects, hybrid FSO/RF schemes offer highly efficient and reliable transmissions [3]. As a result, hybrid FSO/RF-based NTNs are widely recognized for a diverse range of applications, such as post-disaster/emergency communications, wireless backhauling connectivity, and Internet-of-Remote Things (IoRT).

In addition, the NTN architecture with the joint satellite backhauling and Unmanned Aerial Vehicles (UAV) access is notably extensive, particularly in IoRT applications, e.g., emergency search and rescue, police law enforcement, oil/gas/power inspection, and fire prevention and rescue [2]. A satellite establishes the backhaul connections to multiple flying UAV-mounted base stations (BS). This, in turn, raises the issue of resource allocation. Understanding the fading channel characteristics is crucial for developing efficient resource allocation schemes. For instance, more data is allocated to UAVs encountering favorable channel conditions and vice versa. It is worth noting that the extensive studies on designing resource allocation schemes for satellite-assisted multiple backhauled UAVs focused primarily on exploiting RF links, e.g., [2, 4, 5] and references therein. As the FSO links are entirely different from the RF ones, characterized by the pointing error/turbulence fading models and exceptionally high-speed connections [6], it would be crucial to have a well-designed resource allocation scheme for such hybrid FSO/RF-based NTNs. To our knowledge, the performance evaluation of the resource allocation schemes over hybrid FSO/RF-based satellite-assisted multiple backhauled UAVs has yet to be available in the literature.

This letter, for the first time, addresses the performance of a resource allocation scheme over hybrid FSO/RF-based satellite-assisted multiple backhauled UAVs. Notably, the data frame allocation from a low Earth orbit (LEO) satellite to multiple UAVs is considered with the aid of rate adaption. The objective is to allocate the data frames while ensuring the latency fairness constraint as well as targeted Quality of Service (QoS) among multiple UAVs experiencing varying fading channel conditions. Performance metrics, including system outage and achievable throughput, are analyzed. Furthermore, we exploit the feasibility of a case study in Japan networks utilizing the SpaceX's Starlink satellite constellation.

2. System description

2.1 System model

Figure 1 illustrates a Starlink-1487 satellite ($\mathcal{S}$ node), observed on Sep. 23, 2023. We assume this satellite provides backhaul connections for UAV-mounted BSs, denoted as $\mathcal{D}_i$ with $i \in \{1,2\}$, via hybrid FSO/RF links. Here, we assume that one stable UAV located in Aizu-Wakamatsu city (Fukushima) provides Internet access for temporary events, e.g., street festivals or sporting/music events. Also, another UAV in mobility serves in the Tokyo area, e.g., in the context of dynamic ground networks or IoRT applications[1].

In addition, the hybrid FSO/RF links use the hard-switching scheme [1]. In other words, the FSO link, owing to the extremely high data rate, serves as the primary mode. The low-rate RF link serves as the backup mode when the primary FSO link is not favorable, e.g., strong turbulence and

[1] Hanoi University of Science and Technology, Hanoi 100000, Vietnam
[2] School of Computer Science and Engineering, The University of Aizu, Aizuwakamatsu 965-0006, Japan
[a)] hoangle@u-aizu.ac.jp (Corresponding author)

DOI: 10.23919/comex.2023XBL0154
Received November 11, 2023
Accepted November 20, 2023
Publicized January 15, 2024
Copyedited March 1, 2024

[1] This assumption is feasible as the footprint of a Starlink satellite is about 460 km.

Fig. 1 Starlink's satellite network-assisted multiple backhauled UAVs in Japan via hybrid FSO/RF links.

cloud blockage. The link-switching for the hybrid FSO/RF-based $\mathcal{S}$-to-$\mathcal{D}_i$ link is summarized as follows:

$$\text{Link} = \begin{cases} \textbf{FSO} \text{ (primary)}, & \gamma_{\text{Fo},i} \le \gamma_{\text{F},i}, \\ \textbf{RF} \text{ (backup)}, & \gamma_{\text{Fo},i} > \gamma_{\text{F},i}, \gamma_{\text{Ro},i} \le \gamma_{\text{R},i}, \\ \textbf{Outage}, & \gamma_{\text{Fo},i} > \gamma_{\text{F},i}, \gamma_{\text{Ro},i} > \gamma_{\text{R},i}, \end{cases} \quad (1)$$

where $\gamma_{\text{F},i}$ and $\gamma_{\text{R},i}$ are the received signal-to-noise ratio (SNR), while $\gamma_{\text{Fo},i}$ and $\gamma_{\text{Ro},i}$ are the outage thresholds for FSO and RF links, respectively.

2.2 Resource allocation scheme

For data transmission, we consider the downlink from an LEO satellite to multiple UAV-mounted BSs. The data frames are transmitted in fixed-size bursts within equal time slots. Its duration is chosen to be shorter than the channel coherence time. The limitation on the burst size results in the data frame allocation issue among multiple UAVs.

For this purpose, we present the rate adaptation (RA)-aided frame allocation scheme (FAS). The RA-aided FAS aims to allocate the number of data frames (within the fixed-size bursts) while ensuring latency fairness among multiple UAVs. Notably, the number of allocated frames is determined by the data-rate ratio of UAVs. The data rates are adaptively adjusted based on the channel conditions of UAVs to satisfy the QoS, e.g., targeted bit error rate ($\text{BER}_{\text{t},i}^{\mathcal{X}}$) with $\mathcal{X} = \text{F}$ for FSO and $\mathcal{X} = \text{R}$ for RF links. The description of RA-aided FAS can be summarized by two steps, as follows.

- *First,* we need to define transmission modes used for the $\mathcal{D}_i$ node. Using the RA scheme [6], total K modes correspond to K data rates, which is determined based on $K+1$ SNR thresholds, $\left\{\gamma_{k,i}^{\mathcal{X}}\right\}_{k=1}^{K+1}$, i.e.,

$$\gamma_{k,i}^{\mathcal{X}} = \frac{2}{3}\left(2^k - 1\right) \ln\left(\frac{1}{5\text{BER}_{\text{t},i}^{\mathcal{X}}}\right), \quad (2)$$

where $\gamma_{1,i}^{\text{F}} = \gamma_{\text{Fo},i}$ and $\gamma_{1,i}^{\text{R}} = \gamma_{\text{Ro},i}$, while $\gamma_{K+1,i}^{\text{F}} = \infty$ and $\gamma_{K+1,i}^{\text{R}} = \infty$. Given $\gamma_{k,i}^{\mathcal{X}}$, data bit rate is given as

$$R_{i,k}^{\mathcal{X}} = \begin{cases} kR_{\text{F}}, & \gamma_{\text{F},i} \in \left[\gamma_{k,i}^{\text{F}}, \gamma_{k+1,i}^{\text{F}}\right), \text{ FSO link}, \\ kR_{\text{R}}, & \gamma_{\text{R},i} \in \left[\gamma_{k,i}^{\text{R}}, \gamma_{k+1,i}^{\text{R}}\right), \text{ RF link}, \\ 0, & \text{Outage}, \end{cases} \quad (3)$$

where R_{F} and R_{R} are symbol rates of FSO and RF links.

- *Next,* we determine the number of allocated data frames to each UAV based on the latency fairness conditions, i.e., $\tau_i = \tau_j$ with $i, j \in \{1, 2\}$ and $i \neq j$. Here, $\tau_i = t_{\text{prop},i} + t_{\text{trans},i}$, where $t_{\text{prop},i}$ is the propagation delay, and $t_{\text{trans},i}$ is the transmission delay, a function of data rate. The number of allocated frames to the $\mathcal{D}_i$ node is, then, determined as

$$n_i = \left\lfloor \left(\tau_i - t_{\text{prop},i}\right) \frac{N_f}{R_{i,k}^{\mathcal{X}}} \right\rfloor, \quad (4)$$

where N_f (bits) is frame size. Note that, the transmitted burst size from the $\mathcal{S}$ node is given as $n_f = n_1 + n_2$.

3. Hybrid FSO/RF-based backhaul links

This section reviews the hybrid FSO/RF channel models for LEO satellite-to-UAV backhaul links.

3.1 FSO channel model

For the FSO link between the LEO satellite and the UAV$_i$, three critical issues are considered, including cloud attenuation $h_{\text{c},i}$, atmospheric turbulence $h_{\text{t},i}$, and pointing misalignment $h_{\text{p},i}$.

As for the cloud attenuation, the presence of cloud liquid water particles leads to scattering beam propagation and significant power attenuation [1]. The cloud attenuation, $h_{\text{c},i}$, is given as [1, (4)]

$$h_{\text{c},i} = 4.34\left(\frac{3.91}{V_i}\left(\frac{\lambda_{\text{opt}}}{550}\right)^{\delta_i}\right)\frac{H_{\text{c},i}}{\cos(\xi_i)}, \quad (5)$$

where V_i is the visibility, a function of cloud liquid water content (CLWC), i.e., $L_{\text{c},i}$. Additionally, λ_{opt} is the optical wavelength, δ_i is the scattering particle's size distribution, $H_{\text{c},i}$ is the cloud vertical extent, and ξ_i is the zenith angle.

Regarding the atmospheric turbulence, it results in signal power fluctuations at receiver detectors, for which $h_{\text{t},i}$ is described by the Fisher-Snedecor $\mathcal{F}$ model, i.e., [7, (2)]

$$f_{h_{\text{t},i}}\left(h_{\text{t},i}\right) = \frac{a_i^{a_i}(b_i-1)^{b_i}\left(h_{\text{t},i}\right)^{a_i-1}}{\mathcal{B}\left(a_i, b_i\right)\left(a_i h_{\text{t},i} + b_i - 1\right)^{a_i+b_i}}, \quad (6)$$

where $\mathcal{B}(\cdot,\cdot)$ is the beta function, while a_i and b_i are the functions of Rytov variance [7, Section II-B]. Here, the Rytov variance is given as [6, (15)] $\sigma_{\mathrm{R}}^2 = 2.25k_{\mathrm{w}}^{7/6}\sec^{11/6}(\xi_i)\int_{H_{\mathrm{D}_i}}^{H_{\mathrm{S}}} C_n^2(h)(h-H_{\mathrm{D}_i})^{5/6}\mathrm{d}h$, where H_{S} and H_{D_i} are the altitudes of the LEO satellite and the UAV$_i$, respectively. In addition, the turbulence strength, $C_n^2(h)$, is modeled by the Hufnagel-Valley found in [7, (5)].

For UAV hovering-induced misalignment, the generalized model is reported in [6, Section II-B.3], where the PDF of $h_{\mathrm{p},i}$ is given as [6, (17)]

$$f_{h_{\mathrm{p},i}}\left(h_{\mathrm{p},i}\right) = \frac{\varphi_{\mathrm{D},i}^2}{A_{\mathrm{D}_i}^{\varphi_{\mathrm{D},i}^2}}\left(h_{\mathrm{p},i}\right)^{\varphi_{\mathrm{D},i}^2-1},\ 0 \le h_{\mathrm{p},i} \le A_{\mathrm{D}_i}, \quad (7)$$

where A_{D_i} and $\varphi_{\mathrm{D},i}$ are found in [6, (17)].

From (5), (6), and (7), the composite channel coefficient is given as $h_{\mathrm{F},i} = h_{\mathrm{c},i}h_{\mathrm{t},i}h_{\mathrm{p},i}$, and the received SNR is written as $\gamma_{\mathrm{F},i} = \mathfrak{R}_i^2 P_{\mathrm{S}}^2 h_{\mathrm{F},i}^2/\sigma_{\mathrm{n},i}^2$. Here, $\mathfrak{R}_i$ is the UAV detector responsivity, P_{S} is the satellite's transmitted power, and $\sigma_{\mathrm{n},i}^2$ is the receiver noise variance. The PDF of $\gamma_{\mathrm{F},i}$ is then expressed as [8, (12)]

$$f_{\gamma_{\mathrm{F},i}}\left(\gamma_{\mathrm{F},i}\right) = C_0\gamma_{\mathrm{F},i}^{-1}G_{2,2}^{2,1}\left[C_1\gamma_{\mathrm{F},i}\middle|\begin{matrix}1-b_i, 1+\varphi_{\mathrm{D},i}^2\\ a_i, \varphi_{\mathrm{D},i}^2\end{matrix}\right], \quad (8)$$

where $C_0 = \frac{\varphi_{\mathrm{D},i}^2}{2\Gamma(a_i)\Gamma(b_i)}$, $C_1 = \frac{a_i\varphi_{\mathrm{D},i}^2}{(b_i-1)\left(1+\varphi_{\mathrm{D},i}^2\right)\sqrt{\bar{\gamma}_{\mathrm{F},i}}}$, $\bar{\gamma}_{\mathrm{F},i}$ is the average SNR, and $G_{\cdot,\cdot}^{\cdot,\cdot}[\cdot]$ is the Meijer's G-function.

3.2 RF channel model

As reported in [3], the RF link between the LEO satellite and the UAV$_i$ can be modeled by the Rician model, which fits well with the satellite channel model. The PDF and CDF of the channel SNR, denoted as $\gamma_{\mathrm{R},i}$, are given as

$$\begin{aligned} f_{\gamma_{\mathrm{R},i}}\left(\gamma_{\mathrm{R},i}\right) &= D_0 I_0\left(2\sqrt{K_i D_0 \gamma_{\mathrm{R},i}}\right)\exp\left[-D_0\gamma_{\mathrm{R},i} - K_i\right],\\ F_{\gamma_{\mathrm{R},i}}\left(\gamma_{\mathrm{R},i}\right) &= 1 - Q_1\left(\sqrt{2K_i}, \sqrt{2D_0\gamma_{\mathrm{R},i}}\right), \end{aligned} \quad (9)$$

where K_i is the Rician factor, and $D_0 = \frac{K_i+1}{\bar{\gamma}_{\mathrm{R},i}}$ with $\bar{\gamma}_{\mathrm{R},i}$ the average channel SNR. Additionally, $Q_1(\cdot,\cdot)$ is the Marcum Q_1 function, while $I_0(\cdot)$ is the 0-th order modified Bessel function of the first kind.

4. Performance evaluation and selected results

This section presents and discusses outage and throughput performance of the hybrid FSO/RF-based satellite-assisted multiple backhauled UAVs using RA-aided FAS.

4.1 Parameter settings

The parameters used for simulations are as follows:

- *As for the RA scheme,* the symbol rate of R_{F} = 500 Msps and R_{R} = 100 Msps with $K_1 = K_2 = 4$ modes, i.e., BPSK, QPSK, 8-QAM, and 16-QAM.
- *Regarding LEO satellite,* altitude H_{S} = 500 km, optical wavelength λ_{opt} = 1550 nm, zenith angle $\xi_1 = 40°$, $\xi_2 = 30°$, divergence angle θ_{d}^S = 50 μrad, jitter angle $\theta_{\mathrm{Sx}} = \theta_{\mathrm{Sy}}$ = 2 μrad, transmitted power P_{S} = 18 dBm.

Table I Positions of UAVs over the Starlink-1487's PASS duration on 23 September 2023, 19:57:15:00 UTC+9.

Time	Latitude	Longitude	Altitude (m)
Positions of UAV$_1$ in Aizu-Wakamatsu			
0-240	37.52266	139.93899	209.093
Positions of UAV$_2$ in Tokyo			
0	35.678263433	139.714526256	45.3
20	35.676317605	139.716945052	36.5
40	35.674504499	139.719311947	40.2
60	35.672581068	139.721663463	46.2
80	35.670739724	139.724231742	42.3
100	35.668915991	139.726660546	34.7
120	35.667335219	139.729222379	33.6
140	35.665714166	139.731833549	29.9
160	35.663978282	139.734389103	30.3
180	35.662159500	139.736906588	41.2
200	35.660518636	139.739584109	29.4
220	35.659048813	139.742260011	23.9
240	35.658415198	139.745490315	48.2

- *For $\mathcal{D}$ nodes (UAVs),* altitudes H_{D_1} = 150 m and H_{D_2} = 200 m, detector responsivity $\mathfrak{R}_{\mathrm{D}_1} = \mathfrak{R}_{\mathrm{D}_2}$ = 0.9, aperture diameter $D_{\mathrm{D}_1} = D_{\mathrm{D}_2}$ = 10 cm, receiver noise $\sigma_{\mathrm{n},1} = \sigma_{\mathrm{n},2} = 10^{-7}$ A/Hz, and others are found in [6].
- *Other parameters,* ground-level turbulence $\mathrm{C}_n^2(0) = 10^{-14}$ m$^{-2/3}$ ($\mathcal{S}-\mathcal{D}_1$ link) and $\mathrm{C}_n^2(0) = 10^{-13}$ ($\mathcal{S}-\mathcal{D}_2$ link). Time slot duration $\tau_1 = \tau_2$ = 5 ms and data frame size N_f = 975 bytes. For clouds, $H_{\mathrm{c},1} = H_{\mathrm{c},2}$ = 2 km, number cloud droplet concentration M_{c} = 200 cm^{-3}, CLWC L_{c} = 1 mg/m^3. Also, $\overline{\gamma}_{\mathrm{R},1} = \overline{\gamma}_{\mathrm{R},2}$ = 15 dB, $\mathrm{BER}_{\mathrm{t},1} = 10^{-3}$, and $\mathrm{BER}_{\mathrm{t},2} = 10^{-5}$.

For practical consideration, we opt for the STARLINK-1487 satellite over Japan, initiating satellite tracking at the zenith angle of 30° (t = 0 on 23 September 2023, 19:57:15 UTC+9). Also, the UAV's position information, i.e., the longitude, latitude, and elevation, are extracted from Google Earth Pro shown in Table I. The STARLINK-1487 satellite allocates the data frames to two UAVs, including the stable UAV$_1$ located in Aizu-Wakamatsu for a temporary event and the UAV$_2$ in mobility from Tokyo National Stadium (t = 0) to Tokyo Tower (t = 240 seconds) for IoRT applications.

4.2 System outage performance

First, we analyze the system outage performance. It happens when at least one UAV is in the outage mode defined in (1). The outage probability for each $\mathcal{S}$-$\mathcal{D}_i$ is computed as

$$\begin{aligned} P_{\mathrm{o},i} &= P\left(\gamma_{\mathrm{Ro},i} > \gamma_{\mathrm{R},i}\right)P\left(\gamma_{\mathrm{Fo},i} > \gamma_{\mathrm{F},i}\right),\\ &= F_{\gamma_{\mathrm{R},i}}\left(\gamma_{\mathrm{Ro},i}\right)F_{\gamma_{\mathrm{F},i}}\left(\gamma_{\mathrm{Fo},i}\right), \end{aligned} \quad (10)$$

where $\gamma_{\mathrm{Fo,i}}$ and $\gamma_{\mathrm{Ro,i}}$ are found in (2). Besides, $F_{\gamma_{\mathrm{R}},\mathrm{i}}(\cdot)$ and $F_{\gamma_{\mathrm{F}},\mathrm{i}}(\cdot)$ are the channel CDF of RF and FSO link found in Section 3, respectively. Given (10), the system outage performance is expressed by

$$P_{\mathrm{outage}} = 1 - \left(1 - P_{\mathrm{o},1}\right)\left(1 - P_{\mathrm{o},2}\right). \quad (11)$$

Figure 2 confirms the outperformance of the hybrid FSO/RF scheme over FSO links in terms of outage performance. Particularly, we investigate the system outage performance for different channel conditions of the $\mathcal{S}$-$\mathcal{D}_2$ link. Different radial displacement values (UAV positions

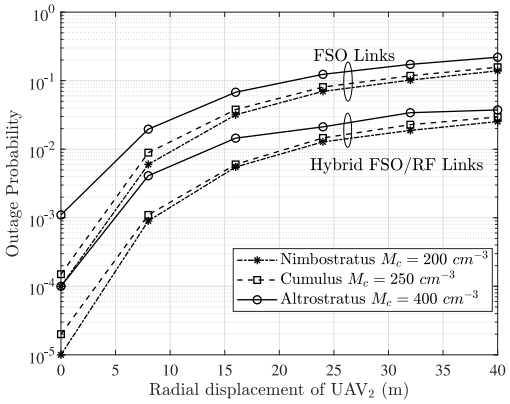

Fig. 2 Outage performance for different channel conditions of $\mathcal{S}$-$\mathcal{D}_2$ link.

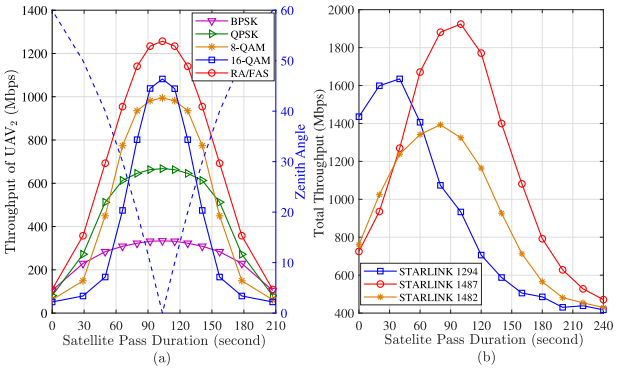

Fig. 3 Achievable throughput performance versus satellite pass duration.

compared to the center of beam footprint) as well as cloud types are taken into account. As is expected, systems using hybrid FSO/RF schemes considerably enhance the outage performance for various channel conditions compared to using FSO links only. Using this figure, we can determine the operational area of UAVs compared to the satellite's beam footprint to retain a targeted outage level. For instance, in the presence of Nimbostratus clouds, the radial displacement of UAVs should be within 20 m to maintain the outage level below 10^{-2}, while it is 10 m when using FSO links only.

4.3 Achievable throughput performance

Next, we investigate the achievable throughput performance over practical Starlink satellite networks. It is defined as the average number of successful data frames per time slot.

Specifically, Fig. 3(a) quantitatively confirms the effectiveness of the RA-aided FAS by comparing its throughput achieved by the UAV$_2$ with that of systems without allocation schemes. These conventional systems employ the single transmission mode, e.g., BPSK only. As is expected, hybrid FSO/RF-based satellite systems using the RA-aided FAS significantly improve the throughput performance over satellite pass duration. This fact can be explained by two noteworthy points: (i) the fixed-rate systems using high modulation orders could achieve high throughput in less severe channel conditions (i.e., with low satellite's zenith angles); (ii) the throughput of such systems is, nonetheless, substantially degraded in more severe channel conditions (i.e., with large zenith angles), for which low modulation orders are preferable leading to low achievable throughput.

Finally, Fig. 3(b) analyzes the total throughput performance with different Starlink satellites, i.e., STARLINK 1294, STARLINK 1482, and STARLINK 1487. To select a proper satellite, the rule of thumb here is that we want to maximize the achievable throughput while retaining a prolonged communication time (to avoid frequent satellite handover). We decide to select the STARLINK 1487, capable of reaching a maximum throughput of 1.9 Gbps and sustaining a throughput level above 800 Mbps for 170 seconds.

5. Conclusion

This letter has addressed the performance of the data frame allocation scheme over hybrid FSO/RF-based satellite-assisted multiple backhauled UAVs. Notably, the RA-aided FAS was employed to allocate data frames effectively while ensuring latency fairness among multiple UAVs experiencing fading channel conditions. Selected illustrative results confirmed the effectiveness of the RA-aided FAS approach over the state-of-the-art solutions in terms of outage and throughput performance. Moreover, the feasibility of a case study over the Japan networks using the Starlink satellite constellation was also explored.

Acknowledgments

This work was supported by the Japan Society for the Promotion of Science (JSPS) KAKENHI Grant Number 23K19124.

References

[1] T.K. Nguyen, C.T. Nguyen, H.D. Le, and A.T. Pham, "TCP over hybrid FSO/RF-based satellite networks in the presence of cloud coverage," *IEICE Commun. Express*, vol. 11, no. 10, pp. 649–654, 2022. DOI: 10.1587/comex.2022XBL0104

[2] Y. Zhu, W. Bai, M. Sheng, J. Li, D. Zhou, and Z. Han, "Joint UAV access and GEO satellite backhaul in IoRT networks: Performance analysis and optimization," *IEEE Internet Things J.*, vol. 8, no. 9, pp. 7126–7139, May 2021. DOI: 10.1109/JIOT.2020.3038691

[3] X. Li, Y. Li, X. Song, L. Shao, and H. Li, "RIS assisted UAV for weather-dependent satellite terrestrial integrated network with hybrid FSO/RF systems," *IEEE Photon. J.*, vol. 15, no. 5, pp. 1–17, Oct. 2023. DOI: 10.1109/JPHOT.2023.3314664

[4] A.H. Arani, P. Hu, and Y. Zhu, "Fairness-aware link optimization for space-terrestrial integrated networks: A reinforcement learning framework," *IEEE Access*, vol. 9, pp. 77624–77636, 2021. DOI: 10.1109/ACCESS.2021.3082862

[5] S. Gu, X. Sun, Z. Yang, T. Huang, W. Xiang, and K. Yu, "Energy-aware coded caching strategy design with resource optimization for satellite-UAV-vehicle-integrated networks," *IEEE Internet Things J.*, vol. 9, no. 8, pp. 5799–5811, April 2022. DOI: 10.1109/JIOT.2021.3065664

[6] H.D. Le, H.D. Nguyen, C.T. Nguyen, and A.T. Pham, "FSO-based space-air-ground integrated vehicular networks: Cooperative HARQ with rate adaptation," *IEEE Trans. Aerosp. Electron. Syst.*, vol. 59, no. 4, pp. 4076–4091, Aug. 2023. DOI: 10.1109/TAES.2023.3236904

[7] H.D. Le, T.V. Nguyen, and A.T. Pham, "Aerial IRS-aided vertical backhaul FSO networks over fisher-snedecor $\mathcal{F}$ turbulence channels," IEEE Int. Conf. Commun. Electron., pp. 133–138, 2022. DOI: 10.1109/ICCE55644.2022.9852053

[8] O.S. Badarneh, R. Derbas, F.S. Almehmadi, F.El Bouanani and S. Muhaidat, "Performance analysis of FSO communications over $\mathcal{F}$ turbulence channels with pointing errors," *IEEE Commun. Lett.*, vol. 25, no. 3, pp. 926–930, March 2021. DOI: 10.1109/ LCOMM.2020.3042489